Ultrafast Excited State Dynamics of the Perylene Radical Cation Generated upon Bimolecular Photoinduced Electron Transfer Reaction

3 AUTHORS, INCLUDING:

Stephane Pages
University of Geneva
19 PUBLICATIONS **313** CITATIONS

Eric Vauthey
University of Geneva
223 PUBLICATIONS **4,338** CITATIONS

Ultrafast Excited State Dynamics of the Perylene Radical Cation Generated upon Bimolecular Photoinduced Electron Transfer Reaction

Stéphane Pagès,[†] Bernhard Lang, and Eric Vauthey*

Department of Physical Chemistry, University of Geneva, 30 quai Ernest-Ansermet, CH-1211 Geneva 4, Switzerland

The ultrafast ground state recovery (GSR) dynamics of the radical cation of perylene, $Pe^{\bullet+}$, generated upon bimolecular photoinduced electron transfer in acetonitrile, has been investigated using pump−pump−probe spectroscopy. With 1,4-dicyanobenzene as electron acceptor, the free ion yield is substantial and the GSR dynamics of $Pe^{\bullet+}$ was found to depend on the time delay between the first and second pump pulses, Δt_{12}, i.e., on the "age" of the ion. At short Δt_{12}, the GSR dynamics is biphasic, and at Δt_{12} larger than about 500 ps, it becomes exponential with a time constant around 3 ps. With *trans*-1,2-dicyanoethylene as acceptor, the free ion yield is essentially zero and the GSR dynamics of $Pe^{\bullet+}$ remains biphasic independently of Δt_{12}. The change of dynamics observed with 1,4-dicyanobenzene is ascribed to the transition from paired to free solvated ion, because in the pair, the excited ion has an additional decay channel to the ground state, i.e., charge recombination followed by charge separation. The rate constants deduced from the analysis of these GSR dynamics are all fully consistent with this hypothesis.

Introduction

Open-shell organic radical ions are known to play a crucial role in many chemical processes. Although the spectroscopy of these species has been rather intensively investigated, especially in low-temperature matrixes,[1,2] very little is known about their excited state dynamics. Excited radical ions have been invoked in phenomena as diverse as the absence of the Marcus inverted region in highly exergonic photoinduced electron transfer reactions,[3] or the emissive diffuse interstellar bands.[4,5] One major reason for the scarcity of information on the photophysics of radical ions is most certainly their lack of fluorescence in the condensed phase, as opposed to the gas phase, where several classes of organic radical cations have been found to fluoresce.[2,6] As reported by Breslin and Fox,[7] most emissions ascribed to radical ions in liquids are actually due to secondary closed-shell products. Consequently, there are only very few reports of genuine fluorescence from radical ions in liquids and in solids.[8−15] Most information on the excited state dynamics of these species has been obtained from transient absorption and related techniques.[16−19] These measurements have revealed very short excited state lifetimes in the 0.5−100 ps range. Although the D_1-D_0 energy gap of most radical ions is relatively small,[20] of the order of 1.5 eV, these decay times are surprisingly short. There is presently no explanation for such ultrafast internal conversion. Nevertheless, it should be noted that only very few radical ions have been investigated so far. The difficulty to perform ultrafast spectroscopy on a chemically unstable species is a major reason for this. Most studies have been performed in solids, namely on cations generated by UV irradiation in boric acid glass at room temperature,[16,18] and on anions and cations formed by γ-irradiation in low-temperature matrixes.[17] The latter approach allows in principle a large variety of radical ions to be investigated. On the other hand, pump−probe measurements require a relatively high photostability of the sample, because the latter cannot be refreshed between two laser pulses. This problem is not present in liquids, but in this case most radical ions are unstable. Some exceptions exist, for example, the radical cations of a few polycyclic aromatic hydrocarbons that are relatively stable in concentrated sulfuric acid.[21] However, sulfuric acid is not a single substance but comprises a dynamic equilibrium involving several species that can influence the excited lifetime of the cation and thus make the interpretation of the data more difficult. Very recently, Okhrimenko et al. reported an investigation of the excited dynamics of the electrochemically generated radical cation of Zn−tetraphenylporphine in acetonitrile.[19] Our approach to investigate the excited state dynamics of such species is to generate them by a photoinduced bimolecular electron transfer (ET) reaction. Several years ago, we measured the ground state recovery (GSR) dynamics of perylene cation generated by ET between perylene in the first singlet excited state and the strong electron acceptor tetracyanoethylene. With the time resolution of the experimental setup used at that time, only an excited state lifetime shorter than 15 ps could be estimated.[16]

We report here on similar pump−pump−probe measurements of the GSR dynamics of perylene cation generated upon photoinduced ET with two different electron acceptors in acetonitrile but performed with a time resolution of the order of 100 fs. Although bimolecular photoinduced ET reactions have been known for a long time to be an efficient way of producing radical ions, the exact nature of the primary ET product is still debated.[22−26] It will be shown that, in some cases, the GSR dynamics of the cation depends on the time delay between the first actinic pulse and the GSR measurement, in other words on the "age" of the ion. Therefore, this approach might become a powerful tool for obtaining a deeper insight into the dynamics of bimolecular ET reactions.

* Corresponding author. E-mail: eric.vauthey@chiphy.unige.ch
† Present address: Centre de Neurophotonique, Centre de Recherche Université Laval Robert-Giffard (CRULRG) 2601, Chemin de la Canardière Beauport (Québec) G1J 2G3 Canada.
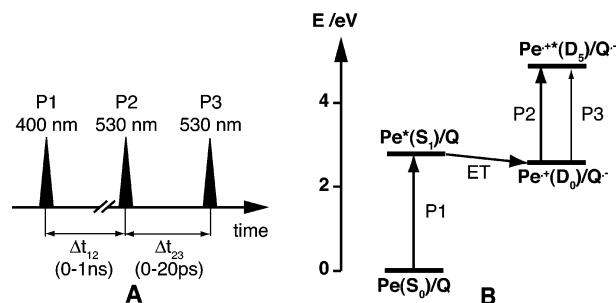
Figure 1. Principle of the pump−pump−probe experiment: (A) pulse sequence; (B) energy level scheme.

Experimental Section

Apparatus. The principle of the pump−pump−probe experiment is illustrated in Figure 1. A first pulse at 400 nm, P1, was used to trigger the photoinduced electron transfer reaction and was generated by frequency doubling a fraction of the output of a 1 kHz amplified Ti:Sapphire system (Spectra-Physics). These 150 fs pulses with energy of about 2 μJ, were focused onto the sample to a spot of about 0.5 mm diameter. Two other pulses, P2 and P3, were used to perform GSR measurements of Pe•+ around 530 nm. They were produced by splitting, with a 20% transmission beam splitter, the output of a homemade noncollinear optical parametric amplifier pumped by another fraction of the Ti:Sapphire amplifier output. These pulses, with duration of about 30 fs after compression and total energy of about 5 μJ, were focused on the sample. The timing between the more intense pulse, P2, and the weaker pulse, P3, was adjusted by sending P3 along a 0−200 ps delay line. On the other hand, the time delay between P1 and P2, Δt_{12}, could be varied between 0 and 1 ns with a longer delay line. The polarization of P2 was parallel to that of P1, and that of P3 was at magic angle. The full width at half-maximum (fwhm) of the P2−P3 cross-correlation at the sample was around 60 fs, and that of the P1−P3 cross-correlation was about 200 fs. Sensitivity better than 0.1 mOD was achieved using reference photodiodes and by chopping the P2 beam at half the laser frequency.

Conventional pump−probe transient absorption (TA) measurements with 400 nm excitation and 530 nm probe were performed with the same setup but with the P2 beam blocked. With this setup, 0−200 ps kinetics could be recorded. Dynamics over larger time delays were measured with a picosecond pump−probe setup based on a passive-active mode-locked Nd:YAG laser (Continuum PY61-10) generating 25−30 ps pulses at 10 Hz. Excitation was performed with the third harmonic at 355 nm, and probing was achieved at magic angle with the second harmonic at 532 nm. The pump energy on the sample was around 0.5 mJ with a spot size of 1.5 mm diameter. The fwhm of the cross-correlation function was around 50 ps.

The fluorescence up-conversion setup has already been described in detail in ref 27. Excitation at 400 nm was carried out with the frequency-doubled output of a Kerr lens mode-locked Ti:Sapphire laser (Tsunami, Spectra-Physics). The fwhm of the instrument response function was 210 fs.

The free ion yields were measured by transient photoconductivity[28] with a cell described in detail previously.[29] Excitation was performed at 355 nm with the above-mentioned Nd:YAG laser. The system benzophenone with 0.02 M 1,4-diazabicyclo-[2,2,2]octane in acetonitrile, which has a free ion yield of unity, was used as a standard.[30]

Samples. Perylene (Pe) was recrystallized from benzene before used. The quencher 1,4-dicyanobenzene (terephthalonitrile, DCB) was recrystallized from ethanol,[31] and *trans*-1,2-

TABLE 1: Best Fit Parameters Obtained from the Multiexponential Analysis of the Fluorescence Decays of Pe with Various Quencher Concentrations in ACN

Q	[Q] (M)	τ_1 (ps)	A_1	τ_2 (ps)	A_2	A_3 (ps)	τ_3 (ps)
DCB	0.05	13	0.13	203	0.19	0.68	968
	0.10	12	0.15	131	0.24	0.61	574
	0.16	9	0.15	98	0.26	0.59	383
DCE	0.04	16	0.24	931	0.76		
	0.10	19	0.21	414	0.79		
	0.20	17	0.40	189	0.60		

dicyanoethylene (fumaronitrile, DCE) was sublimed and then recrystallized from benzene. Acetonitrile (ACN, UV grade) was used as received. All chemicals were from Fluka.

For pump−pump−probe and pump−probe TA measurements at 400 nm, a 1 mm thick cell was used. The solutions, with an absorbance of about 1 at 400 nm, were continuously stirred by Ar-bubbling. For pump−probe TA at 355 nm, the optical path length was 5 mm and the absorbance at this wavelength was 0.5. For fluorescence up-conversion measurements, a 0.4 mm spinning cell was used and the sample absorbance at 400 nm was around 0.1. For photoconductivity measurements, the absorbance of the sample at 355 nm was 0.5 over 1 cm. All sample solutions were bubbled with Ar for 15−20 min before use. No significant sample degradation was observed after the measurements.

Results

Fluorescence. The ET quenching of Pe by DCB and DCE in ACN has first been monitored by time-resolved fluorescence using different quencher concentrations. Because of the relatively poor solubility of DCB in ACN, DCB concentrations larger than 0.16 M could not be investigated. At all concentrations, the fluorescence decay of Pe was found to be nonexponential. With DCE, the decays can be well reproduced with the sum of two exponential functions, and with DCB, three exponential functions have to be used. The resulting best-fit parameters are listed in Table 1. Such nonexponential behavior is characteristic of the so-called transient effect.[32] Several theoretical models of diffusion-assisted reactions can in principle be used to analyze this effect and to estimate various parameters such as the quenching distance or the intrinsic ET rate constant.[33−35] However, the multiexponential analysis is sufficient for the purpose of the present investigation.

Photoconductivity. Transient photoconductivity measurements have also been performed with various quencher concentrations. For Pe/DCB, the free ion yield corrected to 100% quenching was found to amount to 0.30 ± 0.02. On the other hand, a free ion yield of 0.01 ± 0.02, i.e., essentially zero, was measured with Pe/DCE. These values, which are essentially independent of the quencher concentration, agree well with those reported in the literature and obtained using a different technique.[36,37]

Pump−Probe Transient Absorption (TA). The time evolution of Pe•+ population, after excitation of Pe at 400 or 355 nm in the presence of 0.1 M quencher, has been monitored by measuring the absorbance around 530 nm. At this wavelength, Pe•+ exhibits a strong absorption band due to the D_0−D_5 transition,[20,38] whereas neither DCB•− nor DCE•− show any absorption.[20] Finally, ¹Pe* absorbs only very weakly at 530 nm, its main absorption band being centered at 700 nm.[38] Figure 2 shows that the TA time profiles measured with DCB and DCE differ significantly. With DCB, the TA signal rises to a constant value within 1 ns. This rise can be reproduced with a biexponential function with time constants of 29 ps (relative
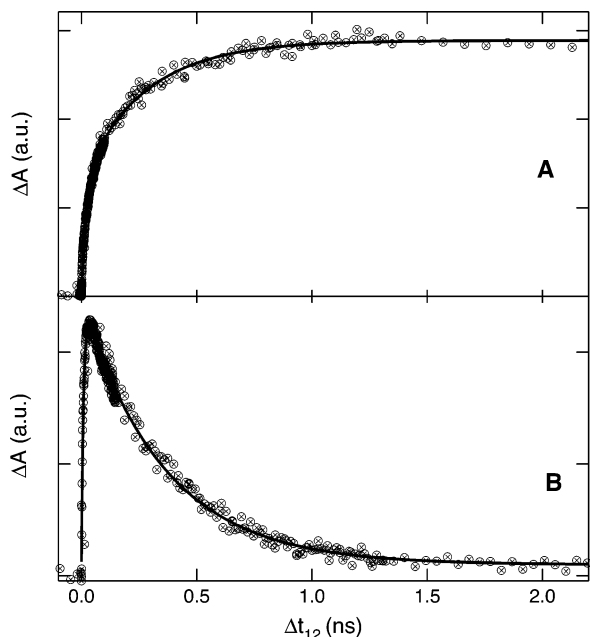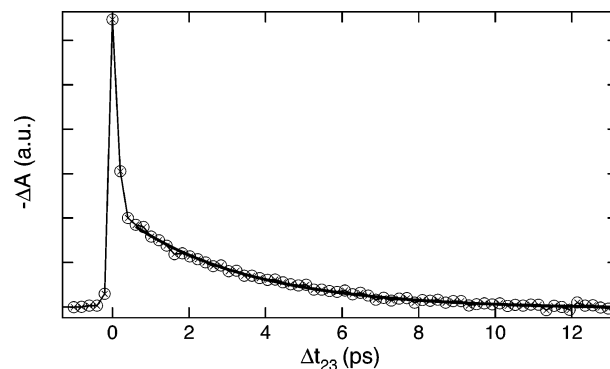
Figure 2. Pump−probe TA profiles at 530 nm measured upon excitation of Pe with 0.1 M DCB (A) and DCE (B) in ACN and best multiexponential fit (solid lines).
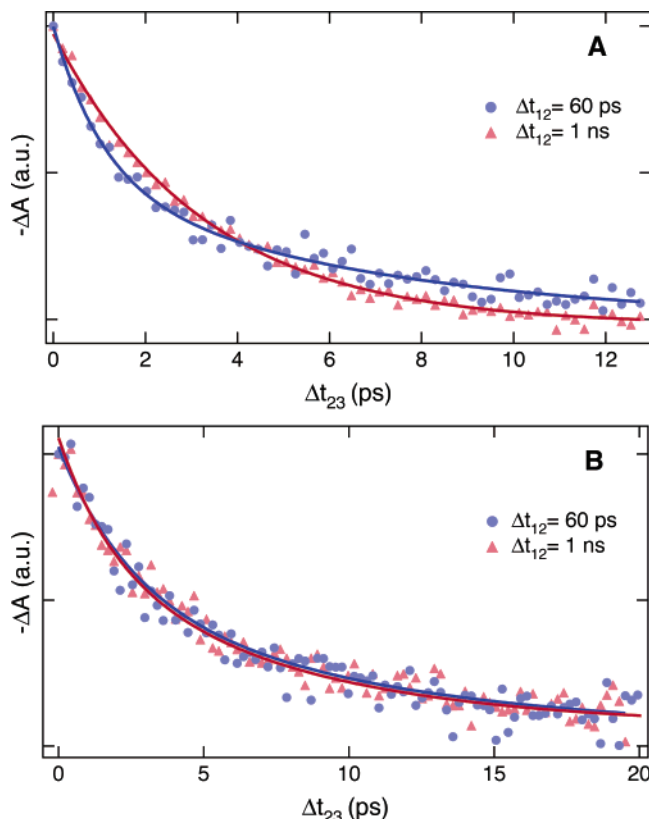

Figure 3. Pump−pump−probe TA profile at 530 nm measured 1 ns after excitation of Pe with 0.1 M DCB in ACN and best single-exponential fit (thick solid line).

amplitude: 0.45) and 280 ps (0.55). The constant TA signal at longer delays can be attributed to the free ion population, which decays by homogeneous recombination on the microsecond time scale. The free ion yield of 0.30 implies that a large fraction of Pe$^{\bullet+}$ population undergoes geminate charge recombination (CR) and that CR and separation of the ion pair into free ions take place on a similar time scale. The absence of a decay component in Figure 2A indicates that this CR process is faster than ET quenching, the latter being relatively slow at 0.1 M DCB.

The TA time profile with DCE exhibits a much faster rise and decays to a value close to zero. The solid line in Figure 2B is the best fit of a biexponential function with a rise time of 10.5 ps and a decay time of 355 ps. These data confirm the negligibly small free ion yield measured by photoconductivity. One can thus conclude that geminate CR of Pe$^{\bullet+}$/DCE$^{\bullet-}$ is much faster than separation into free ions. As the TA decay occurs on the same time scale as ET quenching (see Table 1), the CR rate constant cannot be readily extracted from these data. Some knowledge on the CR dynamics could in principle be obtained by iterative reconvolution of a trial function with the time derivative of the fluorescence decay, as explained in ref 39; this goes, however, beyond the scope of this investigation.

The difference in free ion yield and CR dynamics can be accounted for by the driving force for CR, ΔG_{CR}, which can be calculated as $\Delta G_{CR} = E_{red}(Q) - E_{ox}(Pe)$, where $E_{red}(Q)$ is the reduction potential of the quencher ($E_{red}(DCB) = -1.64$ V vs SCE,[3] and $E_{red}(DCE) = -1.36$ V vs SCE[40]) and $E_{ox}(Pe)$ is the oxidation potential of Pe ($E_{ox}(Pe) = 0.98$ V vs SCE).[37] From this expression, CR of Pe$^{\bullet+}$/DCB$^{\bullet-}$ ($\Delta G_{CR} = -2.62$ eV) is substantially more exergonic than that of Pe$^{\bullet+}$/DCE$^{\bullet-}$ ($\Delta G_{CR} = -2.34$ eV). As CR of such ion pairs is well-known to exhibit the inverted behavior predicted by Marcus ET theory,[38,41−43] it can be expected to be substantially slower with Pe$^{\bullet+}$/DCB$^{\bullet-}$ than with Pe$^{\bullet+}$/DCE$^{\bullet-}$, as observed. Other parameters, such as the electronic coupling constant and the reorganization energy could also contribute to this difference.[44]

Pump−Pump−Probe TA. Figure 3 illustrates the result of a pump−pump−probe experiment with Pe/DCB. This profile was obtained as follows (see Figure 1): 1 ns after the first pump

pulse at 400 nm (P1), a second pump pulse at 530 nm (P2), chopped at half the frequency of the laser, was applied and the absorbance at 530 nm was monitored with a third pulse (P3). Figure 3 is a plot of the change of absorbance at 530 nm induced by P2 as a function of the time delay between P2 and P3, Δt_{23}. In other words, these data correspond to a TA measurement performed on the transient population absorbing at 530 nm. From the sign of the TA, it appears that excitation by P2 leads to a reduced absorbance at 530 nm. This bleach is due to the depletion of the Pe$^{\bullet+}$(D$_0$) population upon D$_0$−D$_5$ excitation, and therefore, the profile depicted in Figure 3 corresponds to the GSR dynamics of Pe$^{\bullet+}$. The initial spike at time zero is due to both a resonant contribution from Pe$^{\bullet+}$, the so-called coherent spike,[45] and a nonresonant contribution from the solvent, namely cross-phase modulation.[46] Its relatively large magnitude is due to the small transient absorbance around 530 nm. As this spike does not contain any information on the population dynamics of Pe$^{\bullet+}$, it has not been included in the analysis. The data following the spike can be well reproduced with an exponential function with a time constant of 3 ps. In many cases, bleach recovery measurements performed in this ultrashort time scale exhibit nonexponential character and substantial probe wavelength dependence.[47,48] This is due to the fact that the repopulated ground state is vibrationally hot and thus the probed absorption band is broader than that of the thermally equilibrated ground state. If the spectrum of the probe pulse is narrower than the probed absorption band, the time profile contains not only the GSR but also the vibrational cooling dynamics. The contribution of vibrational cooling does not appear in the present measurements because the spectrum of the probe pulse (P3) has a width of about 60 nm (fwhm) and thus covers the whole absorption band of Pe$^{\bullet+}$.

Figure 4A shows a comparison of the normalized pump−pump−probe TA time profiles measured with Pe/DCB at two different time delays, Δt_{12}, after excitation with P1. Although the profile measured at $\Delta t_{12} = 1$ ns is monoexponential, that measured at $\Delta t_{12} = 60$ ps cannot be reproduced with less than two exponential functions, with time constants of 1.1 and 6.2 ps. Table 2, which contains the best fit parameters obtained from the analysis of TA time profiles at various Δt_{12}, indicates that the GSR dynamics changes from bi- to monoexponential at $\Delta t_{12} \approx 500$ ps.

Similar pump−pump−probe measurements have been carried out with Pe/DCE. As shown in Figure 4B and in Table 3, the pump−pump−probe TA profiles are biexponential, independently of Δt_{12}. The time constants are also independent of Δt_{12} and are around 2 and 10 ps. It should be noted that at large Δt_{12}, the Pe$^{\bullet+}$ population and thus the signal amplitude are very

Figure 4. Pump−pump−probe TA profiles at 530 nm measured at different time delays Δt_{12} after excitation of Pe with 0.1 M DCB (A) and DCE (B) in ACN and best single or biexponential fits (solid lines).

Figure 5. Energy levels involved in the pump−pump−probe measurements with Pe and DCB in ACN.

TABLE 2: Best Fit Parameters Obtained from the Mono or Biexponential Analysis of the Pump−Pump−Probe TA Profiles Measured with Pe/DCB in ACN at Various Time Delays, Δt_{12}

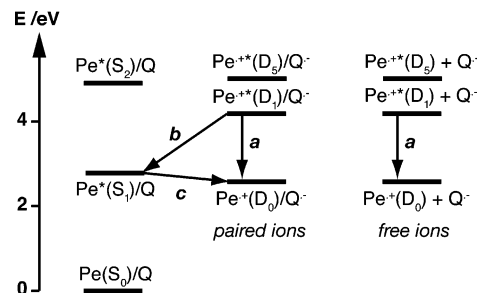| Δt_{12} (ps)	τ_1 (ps)	A_1	τ_2 (ps)	A_2
60	1.1	−0.51	6.2	−0.49
130	0.9	−0.49	5.2	−0.51
200	0.5	−0.29	3.7	−0.71
270	0.4	−0.19	3.8	−0.81
400	0.4	−0.14	3.8	−0.86
530			3.2	−1.0
670			3.1	−1.0
1000			3.0	−1.0

TABLE 3: Best Fit Parameters Obtained from the Mono or Biexponential Analysis of the Pump−Pump−Probe TA Profiles Measured with Pe/DCE in ACN at Various Time Delays, Δt_{12}

Δt_{12} (ps)	τ_1 (ps)	A_1	τ_2 (ps)	A_2
60	12.7	−0.46	2.4	−0.54
150	12.4	−0.47	3.4	−0.53
200	9.6	−0.55	1.7	−0.45
250	10.6	−0.52	2.1	−0.48
350	10.4	−0.41	2.1	−0.59
450	9.4	−0.57	1.8	−0.43
650	12.3	−0.44	3.0	−0.56
1000	11.7	−0.47	2.3	−0.53

small. Therefore, the error on the time constants at short time delay is typically on the order of ±10%, and it rises to about ±25% at longer time delay. Despite this, departure from monoexponential dynamics can be clearly established.

Discussion

The above results reveal that the GSR dynamics of Pe$^{\bullet+}$ depends on the quencher used to oxidize Pe* and, with DCB,

on Δt_{12}, i.e., on the "age" of Pe$^{\bullet+}$. This suggests that the excited cation, Pe$^{\bullet+}$*, interacts with the quencher either in the neutral or in the reduced form. Figure 5 depicts a scheme of the energy levels involved in the pump−pump−probe experiment with DCB. For DCE, the scheme is similar but the ion levels are lower by 0.28 eV. This scheme suggests that there are more deactivation pathways for Pe$^{\bullet+}$* paired with the quencher radical anion, Q$^{\bullet-}$, than for the free solvated Pe$^{\bullet+}$*. Given the very high density of states between the D_5 and D_1 states of Pe$^{\bullet+}$,[49] internal conversion (IC) to D_1 can be expected to be the major deactivation pathway of Pe$^{\bullet+}$*(D_5) paired or free. After this ultrafast IC, the excited paired cation, Pe$^{\bullet+}$*(D_1)/Q$^{\bullet-}$, can either relax to the electronic ground state Pe$^{\bullet+}$(D_0)/Q$^{\bullet-}$ by IC (pathway a) or undergo CR to Pe*(S_1)/Q (pathway b) or to Pe(S_0)/Q. The driving force for the latter process is very large ($\Delta G_{CR} = -4.12$ and -3.84 eV for DCB and DCE, respectively) and corresponds to the far inverted regime. On the other hand, the driving force for CR via pathway b amounts to -1.32 and -1.04 eV for DCB and DCE, respectively. In the latter case, CR is no longer in the inverted region but rather in the barrierless regime and can thus be ultrafast. Therefore, the occurrence of CR to Pe(S_0)/Q can be ruled out. This is further supported by recent investigations evidencing that CR takes place predominantly along the less exergonic pathway.[27,50,51]

The pump−pump−probe TA profiles (Figures 3 and 4) indicate that the Pe$^{\bullet+}$(D_0) state is fully repopulated after excitation with P2, implying that, if CR to Pe*(S_1)/Q is operative, this latter state undergoes a further charge separation to Pe$^{\bullet+}$(D_0)/Q$^{\bullet-}$ (pathway c). This charge separation can in principle be very fast as no diffusion is needed, the reactants being already at the optimal distance. This b−c pathway is no longer possible for free solvated Pe$^{\bullet+}$*(D_1), whose only deactivation channel is IC to the D_0 state (pathway a). Indeed, the second oxidation potential of Pe amounts to 1.59 V vs SCE,[52] and thus a photoinduced ET between Pe$^{\bullet+}$* in either the D_1 or the D_5 state and DCB or DCE is not energetically feasible ($\Delta G_{ET} > 0.6$ eV).

Consequently, the GSR dynamics of Pe$^{\bullet+}$ after excitation to D_5 can be expected to differ depending on whether it is paired with Q$^{\bullet-}$ or it is free. The GSR of Pe$^{\bullet+}$ in the ion pair should be biphasic, with one component due to pathway a and the other to pathway b−c. On the other hand, the GSR of free Pe$^{\bullet+}$ should be monophasic because of the occurrence of a single repopulation pathway, namely pathway a.

We thus ascribe the change of GSR dynamics from biexponential to monoexponential found with Pe/DCB to the dissociation of the Pe$^{\bullet+}$/DCB$^{\bullet-}$ pair into free ions. The observation that, with Pe/DCE, GSR dynamics is biexponential independently of Δt_{12} is totally consistent with the photoconductivity and the pump−probe measurements, both of which indicating a negligibly small free ion yield. With this couple, Pe$^{\bullet+}$ exists only in the paired form.
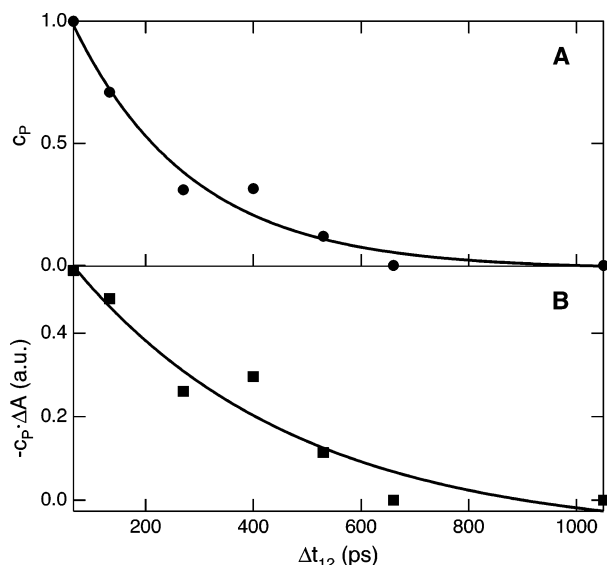
Figure 6. (A) Dependence of c_P, the fraction of the paired Pe$^{\bullet+}$ population, and (B) of c_P multiplied by the transient ion absorbance on the time delay, Δt_{12}, and best exponential fits (solid lines).

To find out whether the time scale connected to the change of GSR dynamics with Pe$^{\bullet+}$/DCB$^{\bullet-}$ is consistent with that of ion pair dissociation, the following function, $f(t)$, has been fitted to the normalized GSR time profiles acquired at different Δt_{12}:

$$f(t) = c_P f_P(t) + c_F f_F(t) \tag{1}$$

where c_P and c_F are the fractions of the paired and free Pe$^{\bullet+}$, respectively, with $c_P + c_F = 1$, and $f_P(t)$ and $f_F(t)$ are functions describing the GSR dynamics of paired and free Pe$^{\bullet+}$, respectively. For $f_P(t)$, the biexponential function reproducing the GSR dynamics at $\Delta t_{12} = 60$ ps was used (see Table 2). At this time delay, it is reasonable to assume that all the Pe$^{\bullet+}$ population is paired. On the other hand, $f_F(t)$ was described as a monoexponential function with a time constant of 3.2 ps. This value was obtained from the GSR dynamics at $\Delta t_{12} = 1$ ns, where Pe$^{\bullet+}$ can be expected to be predominantly free. Equation 1 could be well fitted to all GSR profiles and the variation of c_P with Δt_{12} is shown in Figure 6A. Although the number of points is not very large, the decay of c_P, can be reasonably well reproduced using an exponential function with a time constant of about 200 ps. Physically, c_P is the ratio of the ion pair population over the total ion population. Therefore, the temporal variation of the ion pair population can in principle be recovered by multiplying c_P at a given Δt_{12} by the transient ion absorbance measured at the same delay. The resulting values obtained with the TA profile of Figure 2A suggest an ion pair lifetime on the order of 400 ps (see Figure 6B). In principle, the same information could have been obtained from the initial pump–pump–probe signal intensity before normalization as a function of Δt_{12}. However, as the measurements were not all performed with the same sample and with exactly the same experimental conditions, these initial intensities could not be readily compared.

If the only deactivation pathways of the ion pair population are separation into free ions, with a rate constant k_{sep}, and CR to the neutral ground state, with a rate constant k_{CR}, this 400 ps time constant should correspond to $(k_{sep} + k_{CR})^{-1}$. The use of such rate constants relies on the assumption that CR only occurs when the ions are in contact. If this is not the case, this simple exponential model is no longer valid and more sophisticated models have to be used.[53,54]

In principle, the sum $k_{sep} + k_{CR}$ should also be accessible from the time profile of the transient ion absorption. Indeed, if

the quenching is sufficiently fast, such profiles exhibit a decay that can be well reproduced with an exponential function decaying to a constant value different from zero.[38,44,55] This decay, which supports the use of the exponential model, corresponds to the disappearance of the ion pair population by separation and CR, and the remaining plateau is due to the absorption of the long-lived free ion population. As shown in Figure 2A, such decay is not observed with Pe/DCB in ACN. Indeed, at 0.1 M and even at 0.16 M, the highest DCB concentration that can be achieved in ACN, the quenching is too slow to create an instantaneous ion pair population larger than the final free ion population. Consequently, only a rise to a constant value corresponding to the free ion population is measured.

If the time constant of 400 ps really corresponds to the decay of the ion pair population, then both k_{sep} and k_{CR} can be estimated from this value and from the free ion yield corrected to 100% quenching:

$$\Phi_{ion} = \frac{k_{sep}}{k_{sep} + k_{CR}} \tag{2}$$

From this equation, $k_{sep} = 0.75 \times 10^9$ s^{-1} and $k_{CR} = 1.75 \times 10^9$ s^{-1}. This k_{sep} value is in very good agreement with those reported in the literature for similar systems in ACN and which range from 0.2 to 2.5×10^9 s^{-1}.[38,44,56] Moreover, the value of k_{CR} is also very consistent with those published for CR with a similar driving force. Indeed, for such ion pairs in ACN, $\Delta G_{CR} = -2.62$ eV corresponds to the moderately inverted region where CR typically occurs in the subnanosecond time scale.[44,56]

Consequently, the change of GSR dynamics of Pe$^{\bullet+}$ can be reasonably ascribed to the transition from paired to free ions. Thus, this pump–pump–probe approach can be considered as a new method to distinguish ion pairs and free ions with a high temporal resolution, typically a few picoseconds. This is particularly useful as the electronic absorption spectra of most radical ions in liquids do not change upon pairing. Moreover, time-resolved resonance Raman investigations of bimolecular ET reactions have revealed that ion pairs and free ions have in most cases very similar Raman spectra.[57,58]

The GSR time constants can now be interpreted using the energy level scheme in Figure 5. The GSR rate constant of $1/(3$ ps), obtained at large Δt_{12}, should correspond to k_a, the rate constant of process a, namely IC of Pe$^{\bullet+}$*(D$_1$). The two rate constants associated with the GSR of Pe$^{\bullet+}$ paired with DCB$^{\bullet-}$, $k_1 = \tau_1^{-1} = 0.91$ ps^{-1} and $k_2 = \tau_2^{-1} = 0.16$ ps^{-1} (see Table 2), can be interpreted as follows:

(1) One of these rate constants should corresponds to GSR via IC, which, in the ion pair, should appear with a rate constant $k = k_a + k_b$. If we assume that IC from D$_1$ is not influenced by the presence of DCB$^{\bullet-}$, the value of $k_a = 0.33$ ps^{-1} found with free Pe$^{\bullet+}$*(D$_1$) can be used. Given the large value of k_a, the rate constant $k = k_a + k_b$ can only be associated with k_1, and consequently the rate constant for process b is $k_b = k_1 - k_a = 0.58$ ps^{-1}.

(2) The smaller rate constant, k_2, is related to GSR via processes b–c. As k_2 is substantially smaller than k_b, one can reasonably assume that $k_2 \approx k_c$.

From these values, which are summarized in Table 4, the relative amplitude of the fast GSR component of the paired ions should amount to about 0.4. This agrees rather well with the value of 0.5 found experimentally.

The same reasoning has been repeated with the system Pe/DCE and the resulting values are listed in Table 4. In this case,

TABLE 4: Time Constants (ps) Estimated from the GSR Dynamics of Pe$^{\bullet+}$ Paired with DCB$^{\bullet-}$ or DCE$^{\bullet-}$

	Pe$^{\bullet+}$/DCB$^{\bullet-}$	Pe$^{\bullet+}$/DCE$^{\bullet-}$
k_a^{-1} ^{a}	3	3
k_b^{-1}	1.7	3
k_c^{-1}	6.2	10

^{a} Taken from the GSR measured with Pe$^{\bullet+}$/DCB$^{\bullet-}$ at large Δt_{12}.

however, the uncertainty on k_b is very large as this rate constant varies from 0.07 to 0.34 ps^{-1} depending on the whether k_1 is taken as 0.4 or 0.67 ps^{-1}. Nevertheless, the relative amplitude of the slow and fast GSR components supports a k_b around 0.34 ps^{-1}.

The uncertainty on the rate constants listed in Table 4 is too large to allow a discussion on the differences between DCB and DCE. Nevertheless, one can reasonably examine whether their order of magnitude is realistic. The driving force for process b amounts to -1.32 and -1.04 eV for DCB and DCE, and therefore, according to the literature, CR should be essentially barrierless and thus ultrafast. Time constants of the order of $1-2$ ps have been reported for the CR of ion pairs generated by bimolecular ET quenching of cyanoanthracene derivatives by *N,N*-dimethylaniline in ACN and with a similar driving force ($\Delta G_{CR} = -1.05$ to -1.40 eV).[44] The k_b values found here are thus fully compatible with process *b*.

The time scale for process c can be estimated from the dynamics of fluorescence quenching. The latter was found to be nonexponential because of the so-called transient effect. The shortest decay component can be reasonably associated with donor−acceptor pairs at distances where quenching can occur without significant diffusion. For both DCE and DCB, the shortest time constant measured at various concentrations is of the order of 10 ps (Table 1). This is again in very good agreement with the time constants found for process *c*.

Finally, the GSR time constant of 3 ps found for the free Pe$^{\bullet+}$ is difficult to compare with the literature as there are essentially no data available. Our previous pump−pump−probe measurements already pointed out an excited state lifetime of less than 15 ps in ACN. An excited state lifetime of 17 ps was reported for the electrochemically generated radical cation of zinc−tetraphenylporphine in ACN. This short lifetime was rationalized by the small D_1-D_0 energy gap. For Pe$^{\bullet+}$, the D_1-D_0 gap is somewhat smaller (1.56 eV),[49] and thus a shorter lifetime is reasonable. The GSR dynamics of Pe$^{\bullet+}$ upon D_0-D_5 excitation has already been investigated in concentrated sulfuric acid,[17] in low-temperature rigid matrixes,[17] and in boric acid glass,[16,18] and the reported GSR time constants were all different: around 30 ps in sulfuric acid, 83 and 100 ps in isopentane/butyl chloride and Freon glasses, respectively. Moreover, in boric acid glasses two time constants, namely 20 and 35 ps, have been reported.[16,18] These numbers clearly point out that the GSR of Pe$^{\bullet+}$ is strongly environment dependent. In a previous study, we have suggested that the decay of Pe$^{\bullet+*}$ in acid media was dominated by intermolecular quenching, such as a reversible proton or electron transfer.[17] If such processes indeed occur, the measured GSR time constant cannot be simply equated with the excited state lifetime of Pe$^{\bullet+}$. No such a quenching mechanism can really be envisaged for free Pe$^{\bullet+*}$ in ACN. Indeed, the second oxidation potential of Pe (E_{ox}(Pe$^{\bullet+}$) = 1.59 eV vs SCE) is too high to make the processes Pe$^{\bullet+*}$ + Q → Pe^{2+} + Q$^{\bullet-}$ feasible. Therefore, the 3 ps GSR time constant can be reasonably assumed to reflect the excited state lifetime of free Pe$^{\bullet+}$.

Conclusion

In this investigation, we have shown that the ground state recovery dynamics of perylene cation generated by bimolecular electron transfer quenching in acetonitrile varies as a function of the delay after the initial excitation pulse. As this effect was only observed with a donor/acceptor pair with a large free ion yield, this change is ascribed to the transition from ion pairs to free ions. In the ion pair, the excited cation population can decay both by internal conversion to the ground state and by charge recombination to the excited neutral precursor state. This latter channel is not operative for the free ions. The rate constants deduced from these dynamics in the framework of this hypothesis are all fully consistent and agree well with the literature.

It will be interesting to repeat such measurements with other donor/acceptor pairs. However, as the experimental constraints are quite large, the number of possible candidates is not very large. Nevertheless, other systems and other solvents will be investigated in the near future. A further support for this hypothesis would be the observation of the repopulation of the excited singlet state of perylene. A time-resolved fluorescence investigation with two pump pulses is planned.

This investigation also points out that much more effort has to be invested in the study of the excited state dynamics of radical ions in condensed phase for obtaining a comprehensive picture of their photophysics.

References and Notes

(1) Shida, T.; Haselbach, E.; Bally, T. *Acc. Chem. Res.* **1984**, *17*, 180.
(2) Miller, T. A. *Annu. Rev. Phys. Chem.* **1982**, *33*, 257.
(3) Rehm, D.; Weller, A. *Isr. J. Chem.* **1970**, *8*, 259.
(4) Bohme, D. K. *Chem. Rev.* **1992**, *92*, 1487.
(5) Snow, T. P.; Page, V. L.; Keheyan, Y.; Bierbaum, V. M. *Nature* **1998**, *391*, 259.
(6) Klapstein, D.; Maier, J. P.; Misev, L. In *Molecular Ions: Spectroscopy, Structure and Chemistry*; Miller, T. A., Bondybey, V. E., Eds.; North-Holland: Amsterdam, 1983; p 175.
(7) Breslin, D. T.; Fox, M. A. *J. Phys. Chem.* **1994**, *98*, 408.
(8) Joblin, C.; Salama, F.; Allamandola, L. *J. Chem. Phys.* **1995**, *102*, 9743.
(9) Pankasem, S.; Iu, K. K.; Thomas, J. K. *J. Photochem. Photobiol. A* **1991**, *62*, 53.
(10) Cook, A. R.; Curtiss, L. A.; Miller, J. R. *J. Am. Chem. Soc.* **1997**, *119*, 5729.
(11) Zimmer, K.; Hoppmeier, M.; Schweig, A. *Chem. Phys. Lett.* **1998**, *293*, 366.
(12) Zimmer, K.; Gödicke, B.; Hoppmeier, M.; Meyer, H.; Schweig, A. *Chem. Phys.* **1999**, *248*, 263.
(13) Ichinose, N.; Tanaka, T.; Kawanishi, S.; Suzuki, T.; Endo, K. *J. Phys. Chem. A* **1999**, *103*, 7923.
(14) Ichinose, N.; Kinugasa, J. I.; Hoshiba, T.; Endo, K.; Nakayama, T. *Chem. Phys. Lett.* **2002**, *363*, 270.
(15) Hiratsuka, H.; Yamazaki, T.; Maekawa, Y.; Kajii, Y.; Hikida, T.; Mori, Y. *Chem. Phys. Lett.* **1987**, *139*, 187.
(16) Gumy, J.-C.; Vauthey, E. *J. Phys. Chem. A* **1997**, *101*, 8575.
(17) Brodard, P.; Sarbach, A.; Gumy, J.-C.; Bally, T.; Vauthey, E. *J. Phys. Chem. A* **2001**, *105*, 6594.
(18) Zhao, L.; Lian, R.; Shkrob, I. A.; Crowell, R. A.; Pommeret, S.; Chronister, E. L.; Liu, A. D.; Trifunac, A. D. *J. Phys. Chem.* **2004**, *108*, 25.
(19) Okhrimenko, A. N.; Gusev, A. V.; Rodgers, M. A. *J. Phys. Chem. A* **2005**, *109*, 7653.
(20) Shida, T. *Electronic Absorption Spectra of Radical Ions*; Elsevier: Amsterdam, 1988; Vol. Physical Sciences data 34.
(21) Aalbersberg, W. I.; Hoijtink, G. J.; Mackor, E. L.; Weiland, W. P. *J. Chem. Soc.* **1959**, 3055.
(22) Muller, P.-A.; Högemann, C.; Allonas, X.; Jacques, P.; Vauthey, E. *Chem. Phys. Lett.* **2000**, *326*, 321.
(23) Vauthey, E. *J. Photochem. Photobiol. A* **2006**, *179*, 1.

(24) Mataga, N.; Miyasaka, H. *Adv. Chem. Phys.* **1999**, *107*, 431.

(25) Gould, I. R.; Farid, S. *Acc. Chem. Res.* **1996**, *29*, 522.

(26) Zhong, C.; Zhou, J.; Braun, C. L. *J. Phys. Chem. A* **2004**, *108*, 6842.

(27) Morandeira, A.; Engeli, L.; Vauthey, E. *J. Phys. Chem. A* **2002**, *106*, 4833.

(28) Vauthey, E.; Pilloud, D.; Haselbach, E.; Suppan, P.; Jacques, P. *Chem. Phys. Lett.* **1993**, *215*, 264.

(29) von Raumer, M.; Suppan, P.; Jacques, P. *J. Photochem. Photobiol. A* **1997**, *105*, 21.

(30) Henseler, A.; Vauthey, E. *J. Photochem. Photobiol. A* **1995**, *91*, 7.

(31) Armagero, W. L. F.; Chai, C. L. L. *Purification of Laboratory Chemicals*; Elsevier: Amsterdam, 2003.

(32) Rice, S. A. *Comprehensive Chemical Kinetics, Vol 25. Diffusion-Limited Reactions*; Elsevier: New York, 1985.

(33) Murata, S.; Nishimura, M.; Matsuzaki, S. Y.; Tachiya, M. *Chem. Phys. Lett.* **1994**, *200*, 219.

(34) Burshtein, A. I. *Adv. Chem. Phys.* **2000**, *114*, 419.

(35) Gladkikh, V.; Burshtein, A. I.; Angulo, G.; Pagès, S.; Lang, B.; Vauthey, E. *J. Phys. Chem. A* **2004**, *108*, 6667.

(36) Lewitzka, F.; Löhmannsröben, H.-G. *Z. Phys. Chem.* **1990**, *169*, 203.

(37) Kikuchi, K.; Niwa, T.; Takahashi, Y.; Ikeda, H.; Miyashi, T. *J. Phys. Chem.* **1993**, *97*, 5070.

(38) Mataga, N.; Asahi, T.; Kanda, Y.; Okada, T.; Kakitani, T. *Chem. Phys.* **1988**, *127*, 249.

(39) Pagès, S.; Lang, B.; Vauthey, E. *J. Phys. Chem. A* **2004**, *108*, 549.

(40) Peters, K. S.; Lee, J. *J. Am. Chem. Soc.* **1993**, *115*, 3643.

(41) Marcus, R. A.; Sutin, N. *Biochim. Biophys. Acta* **1985**, *811*, 265.

(42) Gould, I. R.; Ege, D.; Mattes, S. L.; Farid, S. *J. Am. Chem. Soc.* **1987**, *109*, 3794.

(43) Vauthey, E.; Suppan, P.; Haselbach, E. *Helv. Chim. Acta* **1988**, *71*, 93.

(44) Vauthey, E. *J. Phys. Chem. A* **2001**, *105*, 340.

(45) von Jena, A.; Lessing, H. E. *Appl. Phys.* **1979**, *19*, 131.

(46) Ekvall, K.; van der Meulen, P.; Dhollande, C.; Berg, L.-E.; Pommeret, S.; Naskrecki, R.; Mialocq, J.-C. *J. Appl. Phys.* **2000**, *87*, 2340.

(47) Wynne, K.; Galli, C.; Hochstrasser, R. M. *J. Chem. Phys.* **1994**, *100*, 4797.

(48) Son, D. H.; Kambhampati, P.; Kee, T. W.; Barbara, P. F. *J. Phys. Chem. A* **2002**, *106*, 4591.

(49) Hirata, S.; Lee, T. J.; Head-Gordon, M. *J. Chem. Phys.* **1999**, *111*, 8904.

(50) Muller, P.-A.; Vauthey, E. *J. Phys. Chem. A* **2001**, *105*, 5994.

(51) Nicolet, O.; Vauthey, E. *J. Phys. Chem. A* **2003**, *107*, 5894.

(52) Kubota, T.; Kano, K.; Uno, B.; Konse, T. *Bull. Chem. Soc.* **1987**, *60*, 3865.

(53) Burshtein, A. I. *Chem. Phys.* **1999**, *247*, 275.

(54) Burshtein, A. I. *Adv. Chem. Phys.* **2004**, *129*, 105.

(55) Vauthey, E.; Högemann, C.; Allonas, X. *J. Phys. Chem. A* **1998**, *102*, 7362.

(56) Vauthey, E. *J. Phys. Chem. A* **2000**, *104*, 1804.

(57) Vauthey, E.; Phillips, D.; Parker, A. W. *J. Phys. Chem.* **1992**, *96*, 7356.

(58) Vauthey, E.; Parker, A. W.; Phillips, D.; Nohova, B. *J. Am. Chem. Soc.* **1994**, *116*, 9182.